PREPRINT UCRL-78581 Rev. 2

Conf-761108--24

Lawrence Livermore Laboratory

"LASER FUSION EXPERIMENTS AT 2 TW"

E. K. Storm, H. G. Ahlstrom, M. J. Boyle, L. W. Coleman, H. N. Kornblum, R. A. Lerche, D. R. MacQuigg, D. W. Phillion, F. Rainer, V. C. Rupert, V. W. Slivinsky, D. R. Speck, K. G. Tirsell

October 1, 1976

This paper was prepared for submission to the APS Meeting
San Francisco, California, November 15-19, 1976.

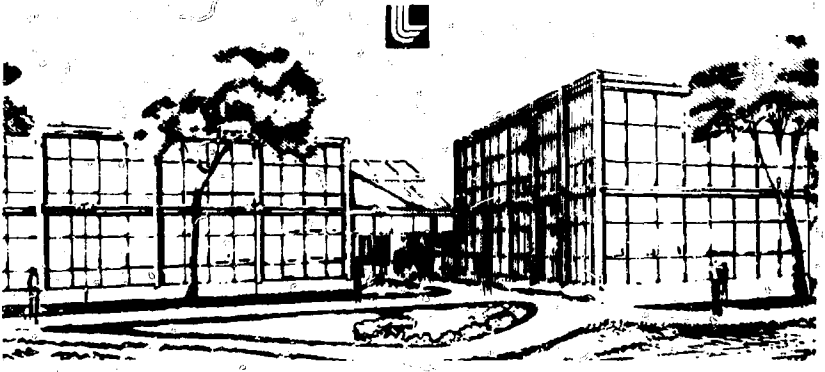

LASER FUSION EXPERIMENTS AT 2 TW *

E. K. Storm, H. G. Ahlstrom, M. J. Boyle, L. W. Coleman,

H. N. Kornblum, R. A. Lerche, D. R. MacQuigg

D. W. Phillion, F. Rainer, V. C. Rupert, V. W. Slivinsky,

D. R. Speck, K. G. Tirsell

Lawrence Livermore Laboratory
University of California
Livermore, California 94550

ABSTRACT

The Lawrence Livermore Laboratory Solid State Laser System, Argus, has successfully performed laser implosion experiments at power levels exceeding 2 TW. D-T filled glass microspheres have been imploded to yield thermonuclear reaction products in excess of 5×10^8 per event. Neutron and α time-of-flight measurements indicate that D-T ion temperatures of ∿ 5-6 keV and a density confinement time product ($n\tau$) of ∿ 1×10^{12} were obtained in these experiments. Typically two 40J, 40 psec pulses of 1.06 μm light were focused on targets using 20 cm aperture f/1 lenses, producing intensities at the target in excess of 10^{16} W/cm^2. An extensive array of diagnostics routinely monitored the laser performance and the laser-target interaction process. Measurements of absorption and asymmetry in both the scattered light distribution and the ion blow off is evidence for non-classical absorption mechanisms and density scale heights of the order of 2 μm or less. The symmetry of the thermonuclear burn region is investigated by monitoring the α-particle flux in several directions, and an experiment to image the thermonuclear burn region is in process. These experiments significantly extend our data base and our understanding of laser induced thermonuclear implosions and the basic laser plasma interaction physics from the 0.4 to 0.7 TW level of previous experiments.

* Work performed under the auspices of the U. S. Energy Research and Development Administration under contract no. W-7405-Eng-48.

LASER FUSION EXPERIMENTS AT 2 TW

The primary goal of the Laser Fusion Program at the Lawrence Livermore Laboratory is to compress to high density and efficiently burn Deuterium-Tritium fuel for the production of thermonuclear energy. As part of the ongoing effort to understand the physics of laser imploded targets, a series of implosion experiments examining a wide range of irradiation geometries and intensities have been performed over the last 2 years.

These include experiments designed to study the basic laser plasma interaction phenomena[1-5] as well as experiments specifically designed to map out and understand the parameter space and physics of laser induced compressions of thermonuclear fuel[6-10]. Early experiments on D-T filled glass microshells[6] and the simple scaling laws developed in that paper indicated that for fixed initial D-T fill, the target performance should increase as $r_o^3 w (E_c/M_T)^{-1/6} \exp(8.11/(E_c/M_T)^{1/3})$. Here r_o is the initial radius, w the wall thickness and E_c/M_T is directly proportional to the final D-T ion temperature, with M_T the target mass in nanograms and E_c the fraction of the absorbed energy in joules which significantly contributes to the implosion, compression and heating of the fuel. This "useful" fraction of the absorbed energy, E_c, is determined roughly by the amount of energy absorbed until the pusher has traversed ~ 30% of the initial target radius (for details, see Reference 8). Since typical pusher velocities are of the order of (2.5-3.5) X 10^7 cm/sec[7,8,11,12] a 90 μm diameter target would clearly find nearly all the energy "useful" for laser pulses with a FWHM ≤ 40 psec. Both to test this hypothesis and to expand our data base, exploding pusher[8] experiments have been performed at the 2 TW level with pulse-

widths (FWHM) of 30-45 psec, using the LLL Argus laser system[13].

A schematic of the Argus laser system, together with an outline of the system performance is shown in Figure 1. In the configuration for these experiments, the Argus laser has produced up to 2.5 TW of power focusable to ~10 μm. The term focusable also signifies that at the target plane there is no noticeable distortion of the temporal pulse shape and that greater than 90% of the energy lies within the low power focal spot. During an experiment, the temporal behavior of the laser power in the target plane is measured using the LLL streak camera[14]. Extensive calorimetry and multiple image cameras also monitor the equivalent target plane[15]. An example of the quality and focusability of the system output is shown in Figures 2a-2e.

The targets used in the experiments were nominally 90 μm diameter SiO_2 microshells with a wall thickness of 0.8 μm and filled with an equimolar mixture of D-T at a density of 2-2.5 mg/cc. A typical target, together with the laser performance and a summary of the results are shown in Figure 3. This is to be compared with a typical result from the 0.4 TW experiments performed with the Janus system[7,16], an example of which is given in Figure 4. We note that (E_c/M_T) has increased by about a factor of 2-3 for the 2 TW Argus experiment as compared to the typical Janus experiment. The absorbed laser energy "useful" in achieving the desired fuel conditions is also reflected in the D-T ion temperature as determined by the α and neutron particle time-of-flight measurements.[9,11] The α particle time-of-flight experiment is depicted in Figure 5. Figure 6 shows an example of the neutron time-of-flight signal[16], compared with the α particle time-of-flight measurement on the same shot.

From Figures 3 and 4 we estimate T_{ion} to be ~ 5.0 keV and ~ 2.0 keV for the Argus and Janus experiments respectively. Using the simple scaling rules

from Reference 8, we would expect the neutron yield to scale as $N \propto r_o^3 w (E_c/M_T)^{-1/6} \exp(8.11/(E_c/M_T)^{1/3})$ with $E_c/M_T = 0.367$ and 0.126 for the two experiments. The ratio of fusion yield for the two experiments is thus estimated to be 146, in reasonable agreement with the experimental value of 124 ± 18.

Again referring to our model, it is clear that the significantly higher fusion yield observed in the Argus experiments is, to first order, dominated by the increase in final D-T ion temperature* caused by the increase in useful specific energy, or E_c/M_T. The α particle energy loss (~ 0.2 MeV) indicate only a slight increase in compression or ρr over the Janus experiments**. In fact, the model implies that for the two experiments listed in Figures 3 and 4, the fusion yield was only increased by a factor of ~ 3.8 due to increased compression.

A more complete comparison of the target performance at the two power levels is given in Figures 7-9. Figure 7 shows the fusion, or neutron yield for the two series of experiments plotted as a function of peak power incident upon the target. Although the neutron yield appears to scale as (peak power)^1, this is not an accurate scaling rule as it fails to take into account the complex interaction of the target mass, the wall thickness and the pulselength.

---

* For example $\langle\sigma v\rangle$ (5.5 keV) / $\langle\sigma v\rangle$ (2.0 keV) ~ 60

** Detailed Lasnex calculations [7] gives ρr of 4.9×10^{-4} and 2.6×10^{-4} gm/cm^2 for the Argus and Janus experiments respectively.

A more appropriate way of displaying the data is shown in Figure 8. Here we plot neutron yield vs. "useful" absorbed energy per target mass, E_c/M_T. The useful fraction of the absorbed energy was determined by the prescription given in Reference 8. In addition, the neutron yield is normalized by (w/w_*) $(r_o/r_*)^3$, where w_* and r_* are the nominal wall thickness (.8 μm) and radius (42.5 μm), respectively.

The solid curve is based upon the set of scaling rules described in Reference 8. Since the model does not predict absolute values, the experimental results given in Figure 4, were chosen as a normalizing point. The model-inferred D-T ion temperatures at other values of E_c/M_T are indicated on the figure and compare reasonably well with the α particle time-of-flight measured values of T_{ion} ~ (1.5 - 2.5) keV for the Janus and ~(4-7) keV for the Argus experiments. Clearly better fitting curves could be drawn through the data set, and additional experiments both at higher and lower values of (E_c/M_T) are needed before a more definitive statement concerning the validity of the scaling rules can be made. Figure 9 shows the D-T ion temperatures as a function both of incident power and (E_c/M_T). The range of the data is indicated by the length of the sides of the boxes. Figure 10 shows the time and space integrated x-ray spectrum for the two experiments. We note that the slope of the superthermal tail, $_{H}$, ($h \nu$ > 10 keV) scales with the incident power to $^{0.405}$, in reasonable agreement with results quoted in References 1 and 3. We also note an increase in the "temperature" one can assign to the thermal portion of the spectrum, from ~ 0.75 to ~ 1 keV. Figure 11 shows the time integrated x-ray microscope image in the 1.5 keV region for the two experiments. The most striking feature is the considerably improved symmetry in the Argus - or 2 TW - experiment. This trend was also noted in the early exploding pusher experiments[7,8] and the series of experiments utilizing the near 4π illumination system[9]. In

both sets of experiments it was observed that the implosion symmetry increased with increasing intensity (W/cm^2) on target, the increased power level is most likely responsible for driving the thermal conduction to heat the target equatorial plane more efficiently, both by providing a larger available heat flux and a larger initial temperature gradient.

Previous experiments[1,4,7,8,18,19] showed that both the scattered 1.06 μm light and the distribution of plasma energy leaving the target exhibited a marked polarization dependence. This effect is also clearly seen in the present experiments. Figure 12 and 13 show the scattered 1.06 μm light and the plasma energy distributions for the Argus experiments. The polarization dependence of the scattered light is seen to be quite strong, with ($I_\perp \leq 4I_\parallel$). The directionality in the distribution of plasma energy is not quite so strong, but is clearly present, and is evidence for resonance absorption. The polarization dependence of the scattered light distributions are consistent with both stimulated Brillouin side scatter of the incident light and resonant absorption. The polarization dependence of the plasma energy, however, is only consistent with the assumption of resonance absorption mechanisms.

By using a computer solution of the wave equation for a plane wave incident at an angle on a one dimensional density profile, one can calculate the state of polarization of the reflected wave for various values of the density scale length and fractional density charge[18]. These calculations are shown in figure 14 together with data from an Argus experiment on an 80 μm glass microshell which was irradiated with 35 Joules on one side and 6 Joules on the other side. Polarimeters[18] looked at light backscattered at an angle of 45° to the incident beam and at a 45° azimuth with respect to the incident laser electric field. The principal axis of the polarimeters were oriented such that if the light were reflected totally in the limit of an infinitely steep density

gradient (metal limit), the degree of polarization would be

$$P = \frac{I_{\parallel} - I_{\perp}}{I_{\parallel} + I_{\perp}} = 1 \qquad (18)$$

The actual experiment shows a degree of polarization of 0.77. Using the numerical calculations for a density jump of $\Delta n/n_c = 1.5$, this corresponds to a density scale height of at most 1.5 μm.

Until the α-particle imaging experiment[20] can give us detailed information on the geometry of the compressed thermonuclear burn region, the α-particle flux is monitored in two directions to give a crude estimate of the uniformity of the compressed DT. The two detectors are at 45° and 90° from the North focusing lens, in the horizontal plane. Both the total yield and the mean α-partcile energy loss (typically between 0.2 and 0.3 MeV) from the two detectors agree to within ± 15% on any given experiment. Thus, within the experimental uncertainty, we have not observed any significant directionality in α particle energy loss in traversing the compressed fuel and pusher.

SUMMARY

Exploding pusher experiments have been performed at the 2 TW/(30-45) psec level utilizing the Argus laser facility. In comparing the results with those obtained at the .4 TW/70 psec level, the following conclusions can be drawn.

1. The increase in target performance is to first order simply given by the increase in absorbed implosion energy per target mass. This quantity increased by a factor of approximately 2-3, resulting in
   a) an increase in peak pusher velocity of $(2\text{-}3)^{1/2}$
   b) a corresponding increase in T_{ion} and
   c) an increase in compression of less than ~ 4
2. The result 1b) was confirmed both by α particle and neutron time-of-flight measurements of the energy spectrum of these reactants.
3. The intensity dependent symmetrization of implosions observed in earlier experiments was confirmed.
4. Polarization dependence of both the scattered light and plasma energy distribution is evidence for the existence of resonance absorption.
5. Measurements of the degree of polaraization of the scattered light indicates density scale heights of 2 μm or less.

REFERENCES

1. K. R. Manes, H. G. Ahlstrom, D. T. Attwood, M. J. Boyle, K. M. Brooks, L. W. Coleman, R. A. Haas, J. F. Holzrichter, H. N. Kornblum, K. J. Pettipiece, D. W. Phillion, F. Rainer, V. C. Rupert, V. W. Slivinsky, E. K. Storm, J. E. Swain, and K. G. Tirsell, "Laser Plasma Interaction Studies at the Lawrence Livermore Laboratory, June 1976, accepted for publication in J. Opt. Soc. Am.

2. R. A. Haas, W. C. Mead, W. L. Kruer, D. W. Phillion, H. N. Kornblum, J. D. Lindl, D. R. MacQuigg, V. C. Rupert, and K. G. Tirsell, "Irradiation of Parylene Disks with a 1.06 μm Laser," LLL UCRL 77930, June 1976, to be published in Phys. Fluids.

3. H. G. Ahlstrom, J. F. Holzrichter, K. R. Manes, E. K. Storm, R. A. Haas, D. W. Phillion, V. C. Rupert, M. J. Boyle, and K. M. Brooks, "Plasma Experiments with 1.06 μm Lasers at the Lawrence Livermore Laboratory," LLL UCRL 77943 (Rev. 1), Sept. 1976, to be published in the proceedings for the Fourth Workshop on Laser Interaction and Related Plasma Phenomena, held at RPI, Troy, New York, Nov. 8-12, 1976.

4. J. T. Larsen, C. E. Max, E. K. Storm, and J. J. Thomson, "Absorption and Conduction in Spherical Laser Targets," LLL UCRL 77901, May 1976.

5. V. W. Slivinsky, H. G. Ahlstrom, K. G. Tirsell, J. T. Larsen, S. S. Glaros, G. B. Zimmerman, and H. D. Shay, "Measurement of the Ion Temperature in Laser-Driven Fusion, "Phys. Rev. Lett., Vol. 35, No. 16, pp. 1083-1085, Oct. 1975.

6. J. F. Holzrichter, E. K. Storm, H. G. Ahlstrom, D. R. Speck, J. E. Swain, L. W. Coleman, C. D. Hendricks, H. N. Kornblum, F. D. Seward, and V. W. Slivinsky, "Laser Implosion and Fusion with Ball-on-Plate and Ball-in-Plate Targets," LLL UCRL 77086, Oct. 1975, also published in Plasma Physics, Vol. 18, pp. 675-680, Jan. 1976.

7. E. K. Storm, J. F. Holzrichter, H. G. Ahlstrom, D. R. Speck, J. E. Swain, L. W. Coleman, C. D. Hendricks, H. N. Kornblum, F. D. Seward, and V. W. Slivinsky, "The Effects of Fill Pressure and Pulse Simultaneity on the Laser-Driven Implosion of DT Filled Glass Microshells," Bull. Am. Phys. Soc., Vol. 20, No. 10, pp. 1266-1267, Oct. 1975, and LLL UCRL 77083.

8. E. K. Storm, H. G. Ahlstrom, and J. F. Holzrichter, "Exploding Pusher Targets Illuminated Using f/1 Lenses at ∿ 0.4 TW," LLL UCRL 78729, Oct. 1976.

9. E. K. Storm, H. G. Ahlstrom, J. A. Monjes, J. E. Swain, V. C. Rupert, and D. W. Phillion, "Exploding Pusher Experiments Utilizing a 4π Illumination System," LLL UCRL 78730, Oct. 1976.

10. K. R. Manes, D. T. Attwood, J. M. Auerbach, J. T. Larsen, D. W. Phillion, and J. E. Swain, "Spherical Microshell Targets Irradiated by the Janus 4π Illumination System," LLL UCRL 78449, Oct. 1976.

11. D. T. Attwood, L. W. Coleman, J. T. Larsen, and E. K. Storm, "Time-Resolved X-Ray Spectral Studies of Laser Compressed Targets, "Phys. Rev. Lett., Vol. 37, No. 9, pp. 499-502, (1976).

12. D. T. Attwood, L. W. Coleman, M. J. Boyle, D. W. Phillion, J. E. Swain, K. R. Manes and J. T. Larsen, "Spatially and Temporally Resolved X-Ray Emission from Imploding Laser Fusion Targets, "LLL UCRL 78434, September 1976.

13. D. R. Speck and W. W. Simmons, "Argus Laser Fusion Facility," LLL UCRL 78438, October 1976.

14. S. W. Thomas, G. R. Tripp, and L. W. Coleman, "Ultrafast Streaking Camera for Picosecond Laser Diagnostics," LLL UCRL 73734, July 1972.

S. W. Thomas, G. E. Phillips, "Comparison of Image-Converter Tubes for Ultra High-Speed Streak Cameras", LLL UCRL 77741.

15. D. R. MacQuigg and D. R. Speak, "Beam Diagnostics on Argus," LLL UCRL 78447, October 1976.

16. R. L. Lerche, L. W. Coleman, J. W. Houghton, D. R. Speck, and E. K. Storm, "DT Ion Temperature Determined from the Neutron Energy Spectrum of Laser Fusion Targets," LLL UCRL 78430, October 1976.

17. J. T. Larsen and A. R. Thiessen, "Computer Simulation of Recent Laser Driven Implosions of Glass Microshells," LLL UCRL 78488.

18. D. W. Phillion and R. L. Lerche, "Scattered Light Evidence for Short Density Scale Heights at Critical Density in Laser-Irradiated Plasma," LLL UCRL 78444, October 1976.

19. D. W. Phillion, R. A. Lerche, V. C. Rupert, K. R. Manes, and S. R. Gunn, "Intensity Distribution of the Scattered 1.06 μm Laser Light and Energy Accounting," Bull. Am. Phys. Soc., Vol. 20, No. 10., pp. 1286, October 1975.

20. K. M. Brooks, H. G. Ahlstrom, H. N. Kornblum, S. S. Glaros, and V. W. Slivinsky, "Pinhole Imaging of Laser Produced 3.52 MeV Thermonuclear Alpha Particles, LLL UCRL 78417.

FIGURE CAPTIONS

1. The Argus laser and its performance.

2a. Argus incident beam diagnostics.

b. Near field camera - laser output energy distributions.

c. Argus north beam - typical high power energy distribution at target plane.

d. Power on target vs. time - Argus north beam.

e. Argus north beam - 158 microns inside f/1 focus.

3. Argus experiment (shot number 36130812).

4. Janus experiment (shot number 75060402).

5. Alpha particle time-of-flight experiment.

6. Neutron and alpha time-of-flight measurements determine the fuel temperature.

7. Neutron yield versus peak power.

8. Neutron yield as a function of useful specific energy.

9. D-T ion temperature increases with peak laser power and useful energy/target mass.

10a. X-Ray spectrum for 0.4 and 2 TW experiments.

b. X-Ray spectrum for 0.4 and 2 TW experiments.

11. The heating and implosion symmetry is a function of the intensity.

12. Irradiation of microshells with f/1 focusing lenses show a strong polarization dependence of the scattered light as well as the particle and x-ray energies.

13. With f/1 focusing optics a strong polarization dependence of the ion and x-ray flux is apparent.

14. Determination of the scale height by polarimetry.

THE ARGUS LASER AND ITS PERFORMANCE

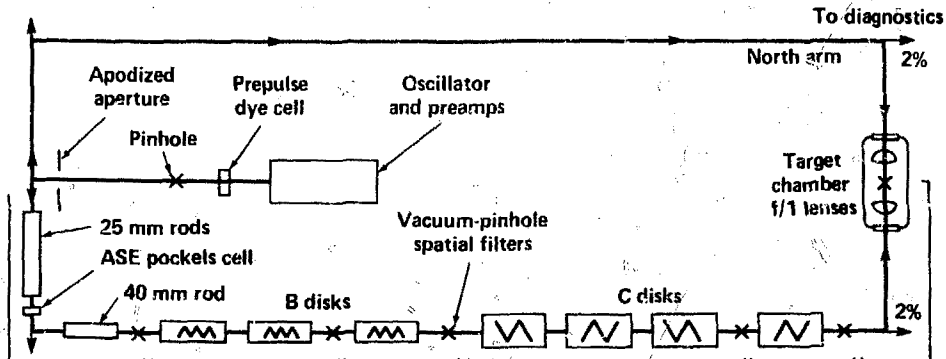

Section	1	2	3	4	5	6	
Beam diameter	40.0	85.0	85.0	200.0	200.0	200.0	mm
B integral							
Small scale	0.6	0.7	1.2	2.1	1.8	1.9	
Whole beam	0.6	1.3	2.5	4.6	6.4	8.3	
Focusable power per arm	0.005	0.050	0.175	0.85	1.34	1.26	TW

FILL FACTOR = 0.5

11/76

Figure 1

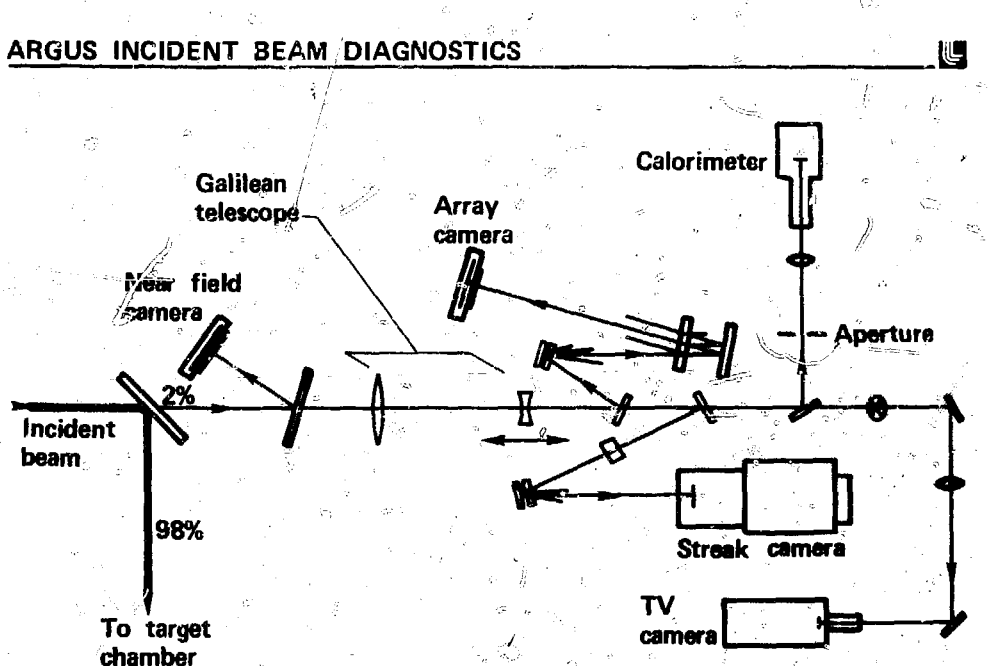
ARGUS INCIDENT BEAM DIAGNOSTICS
Galilean telescope
Array camera
Calorimeter
Near field camera
Aperture
2%
Incident beam
98%
Streak camera
TV camera
To target chamber
8/76

Figure 2a

NEAR FIELD CAMERA – LASER OUTPUT ENERGY DISTRIBUTIONS

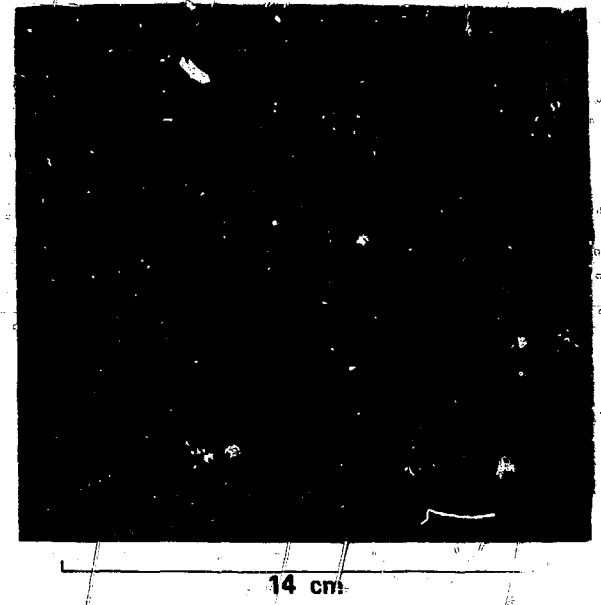

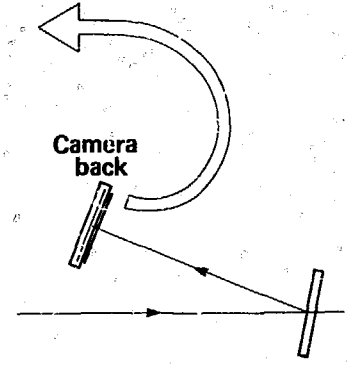

8/76

Figure 2b

ARGUS NORTH BEAM – TYPICAL HIGH POWER ENERGY DISTRIBUTION AT TARGET PLANE

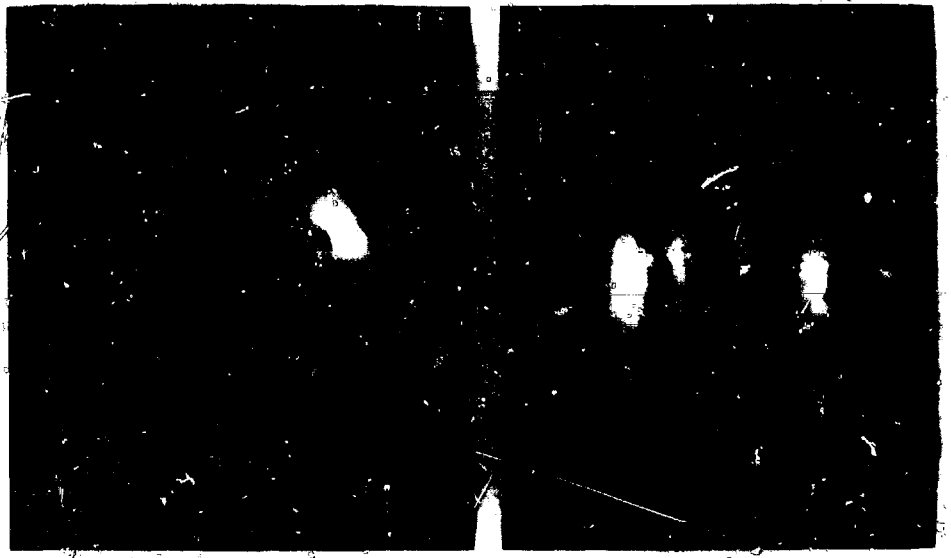

Array camera record
time integrated

Streak camera record
time resolved

Shot 36060801 70 Joules 63 psec 1.1 TW 7×10^7 neutrons
158 microns inside f/1 focus

8-76

Figure 2c

POWER ON TARGET VS TIME – ARGUS NORTH BEAM

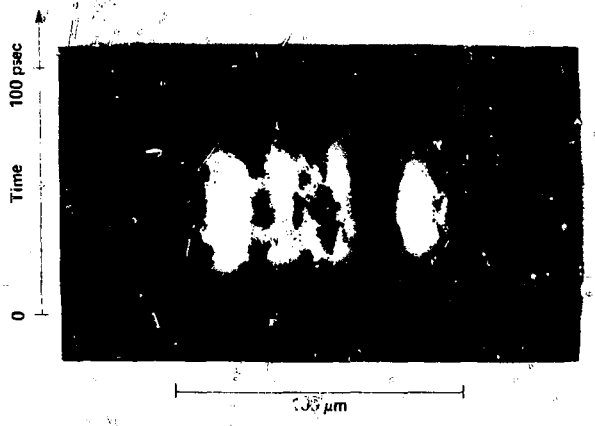

Streak camera record of equivalent target plane

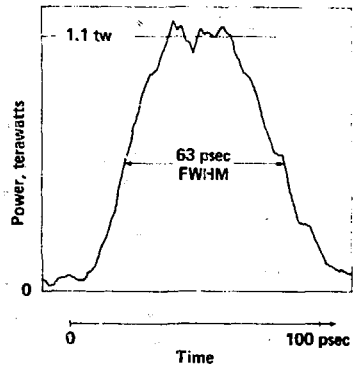

Shot 36060801 70 Joules 63 psec 7×10^7 neutrons 8/76

Figure 2d

ARGUS NORTH BEAM — 158 MICRONS INSIDE f/1 FOCUS

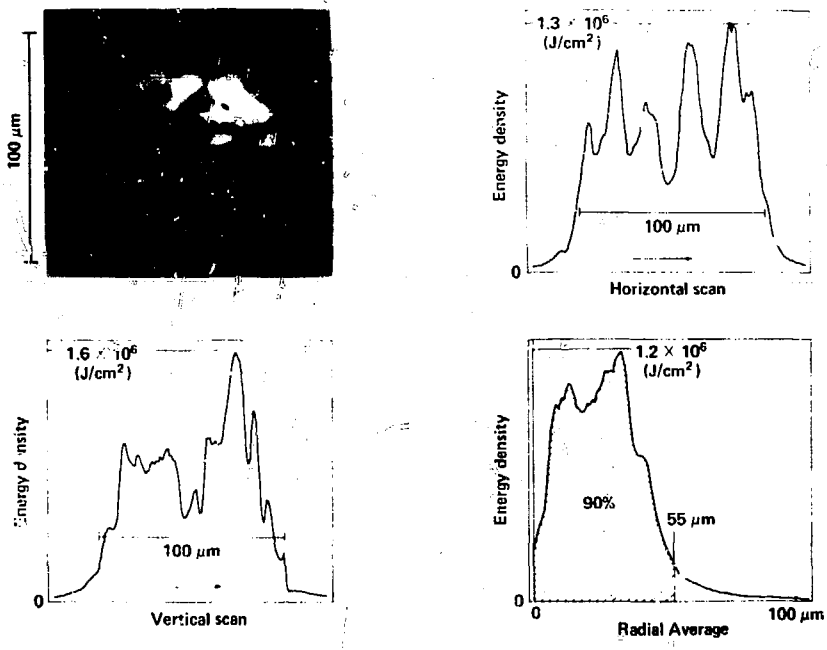

Shot 36060801 70 Joules 63 psec 1.1 tw 7×10^7 neutrons 8-76

Figure 2e

ARGUS EXPERIMENT

Shot number 36100812

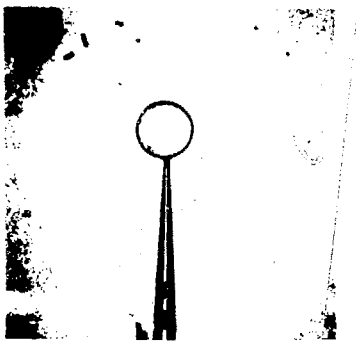

Target characteristics

Diameter = 87 μm
Wall thickness = 0.95 μm
D-T fill = 2.3 mg/cc

Laser performance

96 Joules/38 psec FWHM
⇒ 2.5 TW

Target performance:

Energy absorbed E_a = 24 Joules (~25%)
Useful specific energy E_c/M_T = 0.367 J/ng
Thermonuclear yield $N(n) = (5.5 \pm 1) \times 10^8$ $N(\alpha) = (5.9 \pm 0.3) \times 10^8$
D-T ion temperature a) from α time-of-flight $T_{ion} \lesssim 4.8$ keV
b) from neutron time-of-flight $T_{ion} \lesssim 5.4$ keV
Integrated x-ray emission (0.3 keV $\lesssim h\nu \lesssim$ 17 keV) E_x = 2 J

11/76

Figure 3

JANUS EXPERIMENT

SHOT NUMBER 75060402

TARGET CHARACTERISTICS: DIAMETER = 86.5 μm
WALL THICKNESS = 0.70 μm
D-T FILL = 2.5 mg/cc

LASER PERFORMANCE: 28.3 JOULES
70 PSEC FWHM $\Rightarrow$ 0.40 TW

TARGET PERFORMANCE:

ENERGY ABSORBED E_A = 6.4 J (26%)

"USEFUL" ABSORBED ENERGY/TARGET MASS E_C/M_T = 0.126

(BASED ON THE MODEL FROM REFERENCE 8)

THERMO NUCLEAR YIELD $N(N) = (4.6 \pm 0.4) \times 10^6$ $N(\alpha) = (4.6 \pm 0.5) \times 10^6$

D-T ION TEMPERATURE FROM α TIME-OF-FLIGHT $T_I \lesssim 2.0$ KEV

INTEGRATED X-RAY EMISSION (0.3 KEV $\lesssim h\nu \lesssim$ 17 KEV) $E_X \simeq 0.4$ J

Figure 4

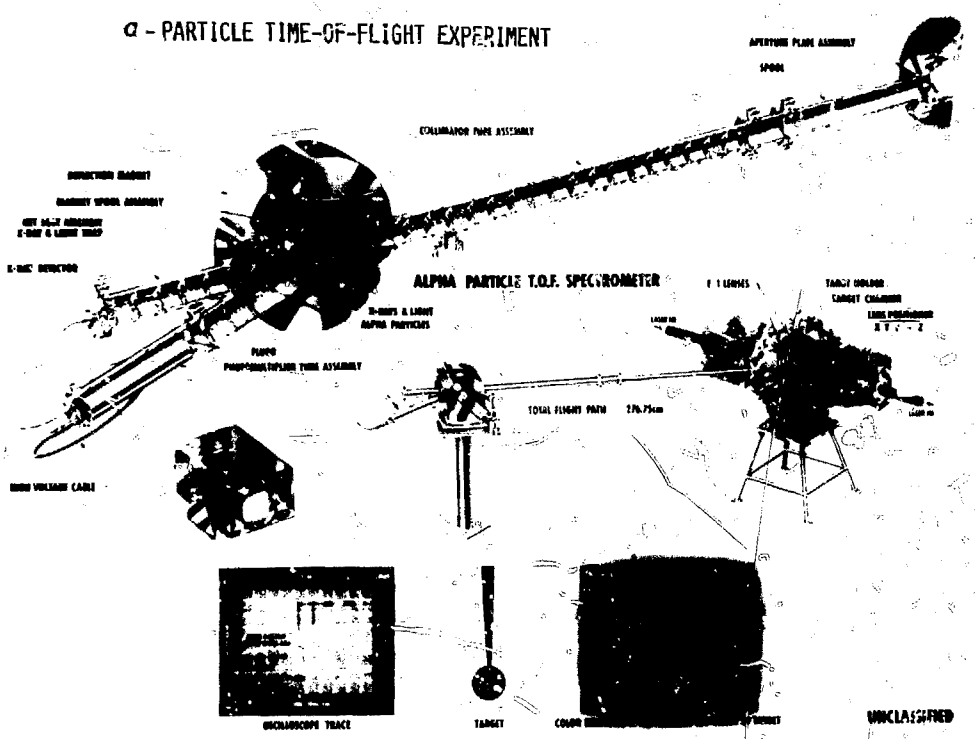
α - PARTICLE TIME-OF-FLIGHT EXPERIMENT
APERTURE PLATE ASSEMBLY
SPOOL
COLLIMATOR PLATE ASSEMBLY
ALPHA PARTICLE T.O.F. SPECTROMETER
TOTAL FLIGHT PATH
OSCILLOSCOPE TRACE
TARGET
UNCLASSIFIED

Figure 5

NEUTRON AND α TIME-OF-FLIGHT MEASUREMENTS DETERMINE THE FUEL TEMPERATURE

Neutrons

E_{peak} = 14.03 MeV
ΔE = 458 keV
$\Rightarrow T_i \leq 6.7$ keV
163 neutrons reacting with detector

Target: SiO_2 microballoon, 105 μm diameter, 0.78 μm wall, 1.7 mg/cc D-T

Laser: 104 Joules, 40 ps FWHM (2.6 TW)

α-particles

E_{peak} = 3.30 MeV
ΔE = 410 keV
$\Rightarrow T_i \leq 5.4$ keV
94 α's reacting with detector

Shot: 36[illegible]1610

Figure 6

NEUTRON YIELD VERSUS PEAK POWER

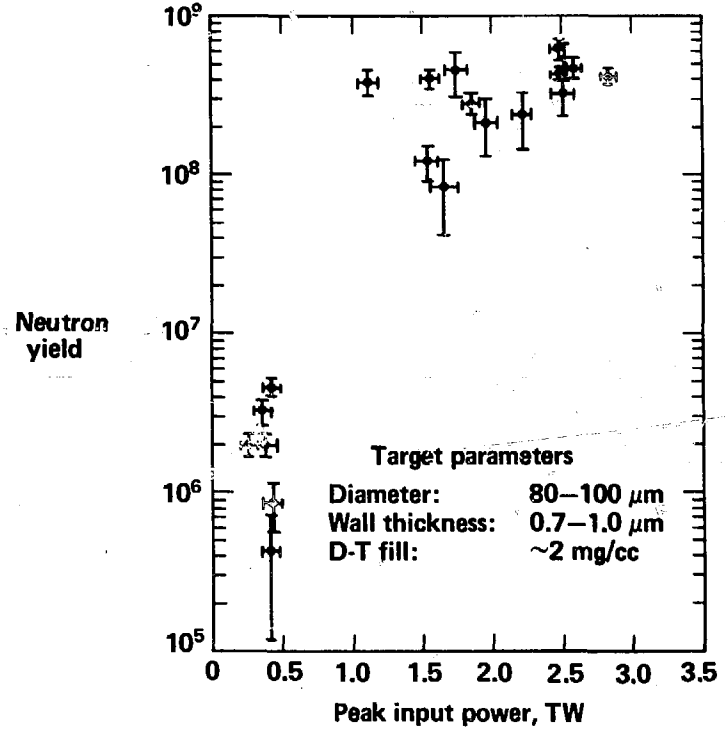

11/76

Figure 7

NEUTRON YIELD AS A FUNCTION OF USEFUL SPECIFIC ENERGY

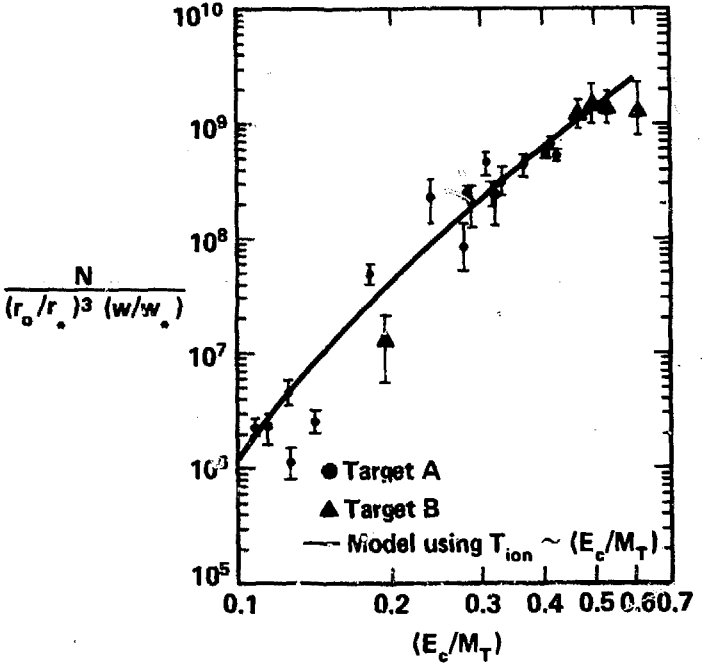

1/77

Figure 8

D-T ION TEMPERATURE INCREASES WITH PEAK LASER POWER AND USEFUL ENERGY/TARGET MASS

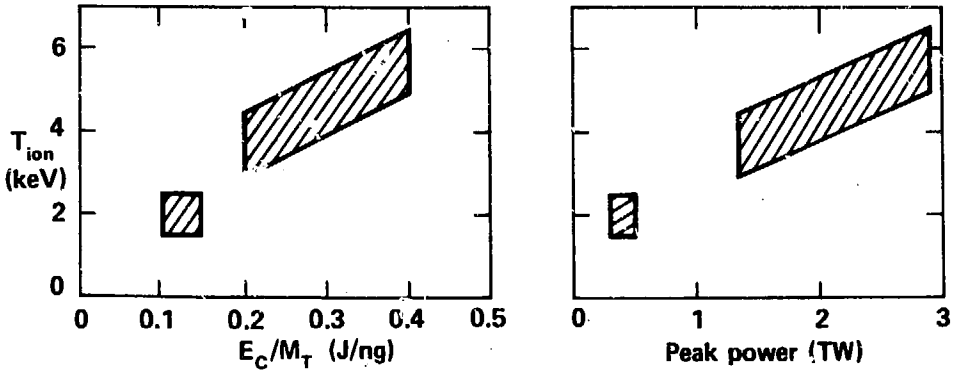

11/76

Figure 9

X-RAY SPECTRUM FOR 0.4 AND 2 TW EXPERIMENTS

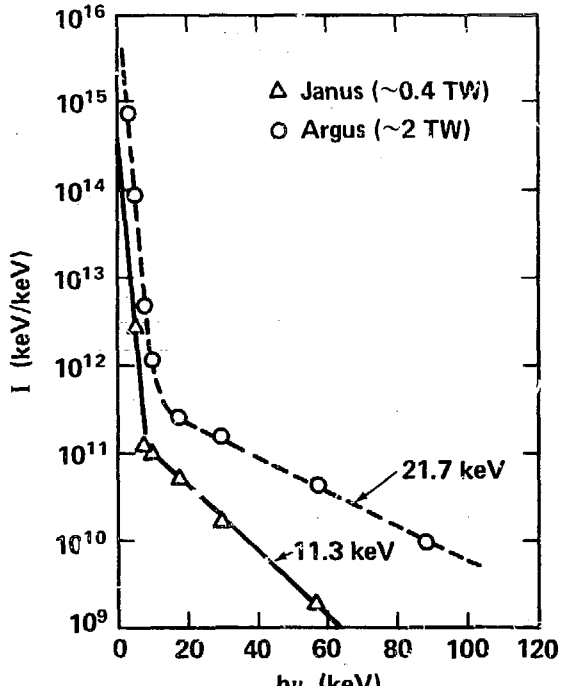

11/76

Figure 10a

X-RAY SPECTRUM FOR 0.4 AND 2 TW EXPERIMENTS

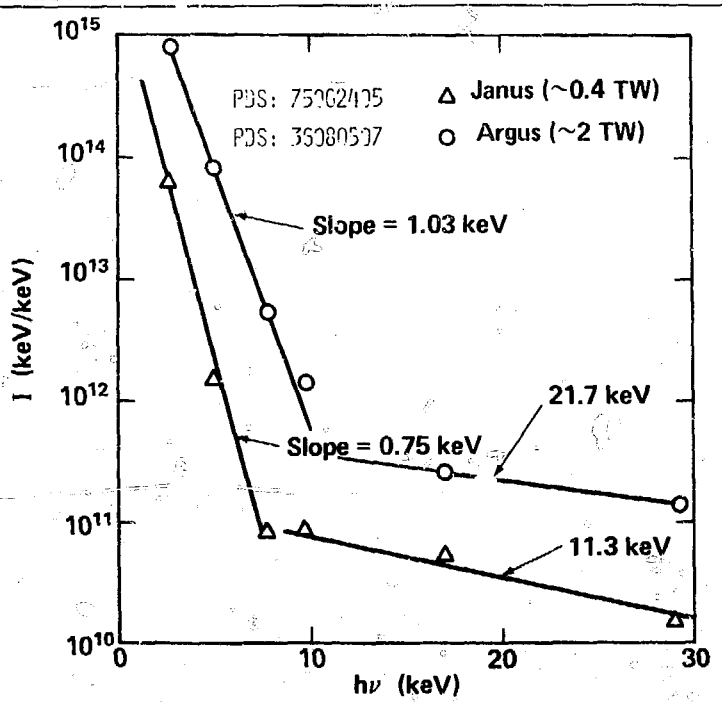

11/76

Figure 10b

THE HEATING AND IMPLOSION SYMMETRY IS A FUNCTION OF THE INTENSITY

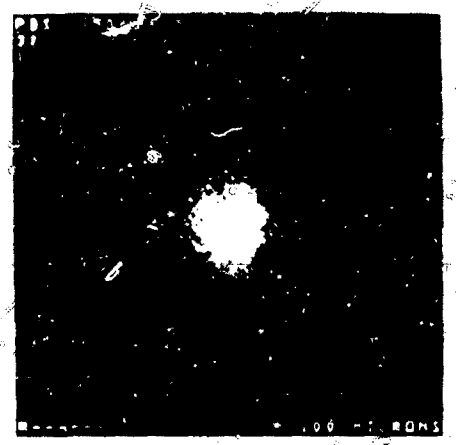

Janus
0.4 TW

Argus
2 TW

$E_{x\text{-}ray} = 1.5$ keV

9-76

Figure 11

IRRADIATION OF MICROSHELLS WITH F/1 FOCUSING LENSES SHOW A STRONG POLARIZATION DEPENDENCE OF THE SCATTERED LIGHT AS WELL AS THE PARTICLE AND X-RAY ENERGIES

Shot 36080507: Incident energy 80 J 49ps
Neutron yield 1.5 X 10^8

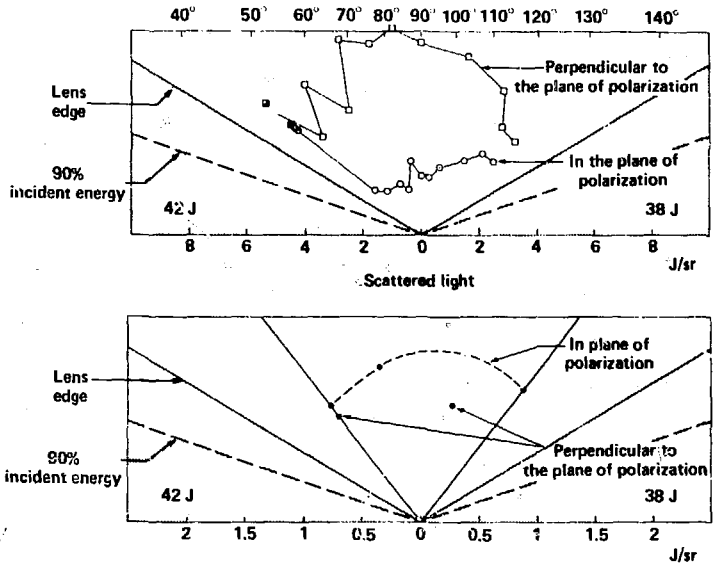

11/76

Figure 12

WITH f/1 FOCUSING OPTICS A STRONG POLARIZATION DEPENDANCE OF THE ION AND X-RAY FLUX IS APPARENT

Shot 36091408

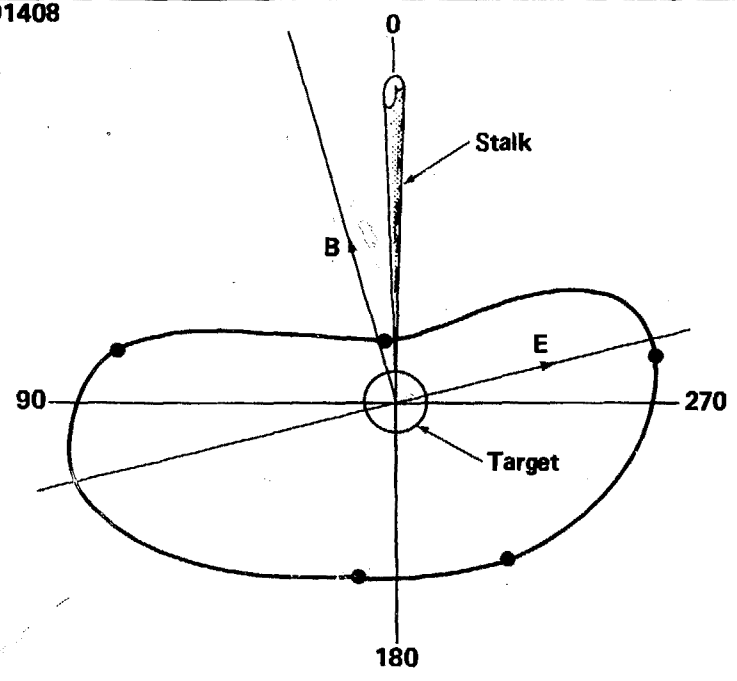

9/76

Figure 13

DETERMINATION OF THE SCALE HEIGHT BY POLARIMETRY

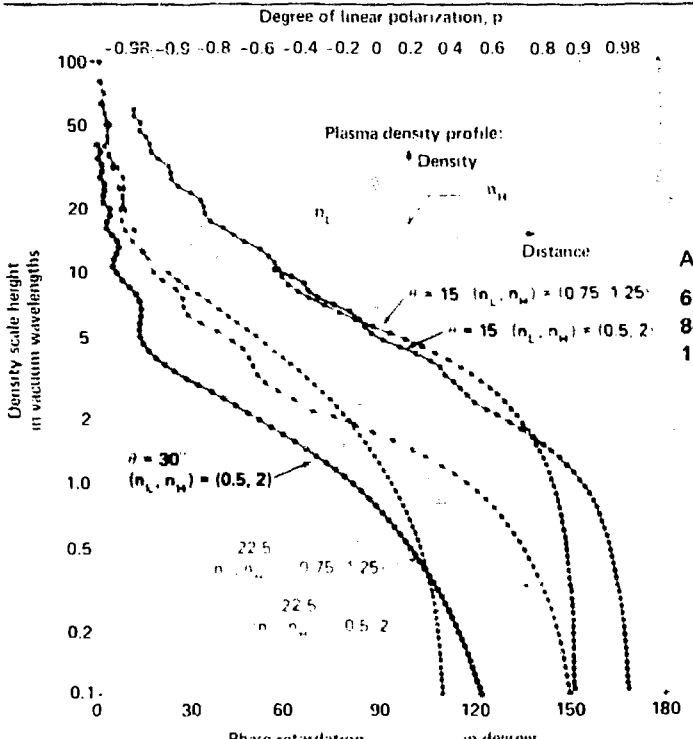

ARGUS shot =36080406

6.4J (N)/40.6J (S) incident
84 μ OD, 0.8 μ WT, 1.9 mg/cm^3 DT
$1.3 \cdot 10^7$ neutrons

p = 0.77

Figure 14